Massive destabilization of an Arctic ice cap

Michael J. Willis [a,b,*], Whyjay Zheng [b], William J. Durkin IV [b], Matthew E. Pritchard [b],
Joan M. Ramage [c], Julian A. Dowdeswell [d], Toby J. Benham [d], Robin P. Bassford [e],
Leigh A. Stearns [f], Andrey F. Glazovsky [g], Yuri Y. Macheret [g], Claire C. Porter [h]

[a] Cooperative Institute for Research in Environmental Sciences (CIRES), University of Colorado, Boulder, CO, 80309, USA
[b] Department of Earth and Atmospheric Sciences, Cornell University, Ithaca, NY, 14853, USA
[c] Department of Earth and Environmental Sciences, Lehigh University, Bethlehem, PA, 18015, USA
[d] Scott Polar Research Institute, University of Cambridge, Cambridge, CB2 1ER, UK
[e] Hardenhuish School, Chippenham, Wiltshire, SN14 6RJ, UK
[f] Department of Geology, University of Kansas, Lawrence, KS 66045, USA
[g] Institute of Geography, Russian Academy of Sciences, Staromonetny 29, 119107, Moscow, Russia
[h] Polar Geospatial Center, University of Minnesota, Saint Paul, MN, 55108, USA

ARTICLE INFO

ABSTRACT

Ice caps that are mostly frozen at the bedrock-ice interface are thought to be stable and respond slowly to changes in climate. We use remote sensing to measure velocity and thickness changes that occur when the margin of the largely cold-based Vavilov Ice Cap in the Russian High Arctic advances over weak marine sediments. We show that cold-based to polythermal glacier systems with no previous history of surging may evolve with unexpected and unprecedented speed when their basal boundary conditions change, resulting in very large dynamic ice mass losses (an increase in annual mass loss by a factor of ∼100) over a few years. We question the future long-term stability of cold and polythermal polar ice caps, many of which terminate in marine waters as the climate becomes warmer and wetter in the polar regions.

Significance statement: A tipping point is reached as a largely cold-based ice-cap outlet glacier with no previous history of surges advanced over low-friction marine sediments, causing it to accelerate and thin.

1. Introduction

High latitude cold and polythermal glaciers and ice caps cover ∼450,000 km^2 of the Earth's surface (Gardner et al., 2013) and hold ∼0.30 m of potential sea-level rise (Radić et al., 2014). These glaciers occur in polar desert environments that are characterized by sub-freezing average temperatures and low rates of annual precipitation, typically below 250 mm/yr. Cold-based glaciers are frozen to their bed and flow by internal deformation at rates of only a few meters per year. Ice in temperate glaciers is at the melting point throughout the body of the glacier with the glacier moving primarily by sliding. Polythermal glaciers are intermediate, with some parts of the glacier cold-based and other

parts wet and temperate. Some 2,300 polythermal and temperate glaciers around the planet surge, undergoing short-duration accelerations in ice flow (Copland et al., 2003; Grant et al., 2009a; Jiskoot et al., 2000; Sevestre and Benn, 2015) that manifest as a rapid glacier advance, thinning in the accumulation area and thickening at the ice front. These surge mechanisms are not understood fully, but are thought to be driven by cyclic oscillations in basal hydraulic conditions (Clarke, 1991; Harrison and Post, 2003; Kamb et al., 1985; Raymond, 1987), controlled by a combination of sub-glacial geometry, the local climate and/or the basal thermal regime (e.g. Bindschadler et al., 1976; Dunse et al., 2015; Murray et al., 2003). Surges result in a rapid transfer of ice mass from the accumulation zone of a glacier to the ablation zone and often leave a long-term glaciological and/or geomorphological signature, such as looped moraines, that can be used to identify surging glaciers in their quiescent phase (Grant et al., 2009b; Ottesen et al., 2017; Ottesen and Dowdeswell, 2006). The quiescent phase is usually an order of magnitude longer in duration than the active phase. Here we present the first observations of an outlet glacier at a largely cold-based ice cap, the Vavilov Ice Cap on October Revolution Island, Severnaya Zemlya archipelago in the Russian High Arctic [Fig. 1], that is undergoing extraordinary ac-
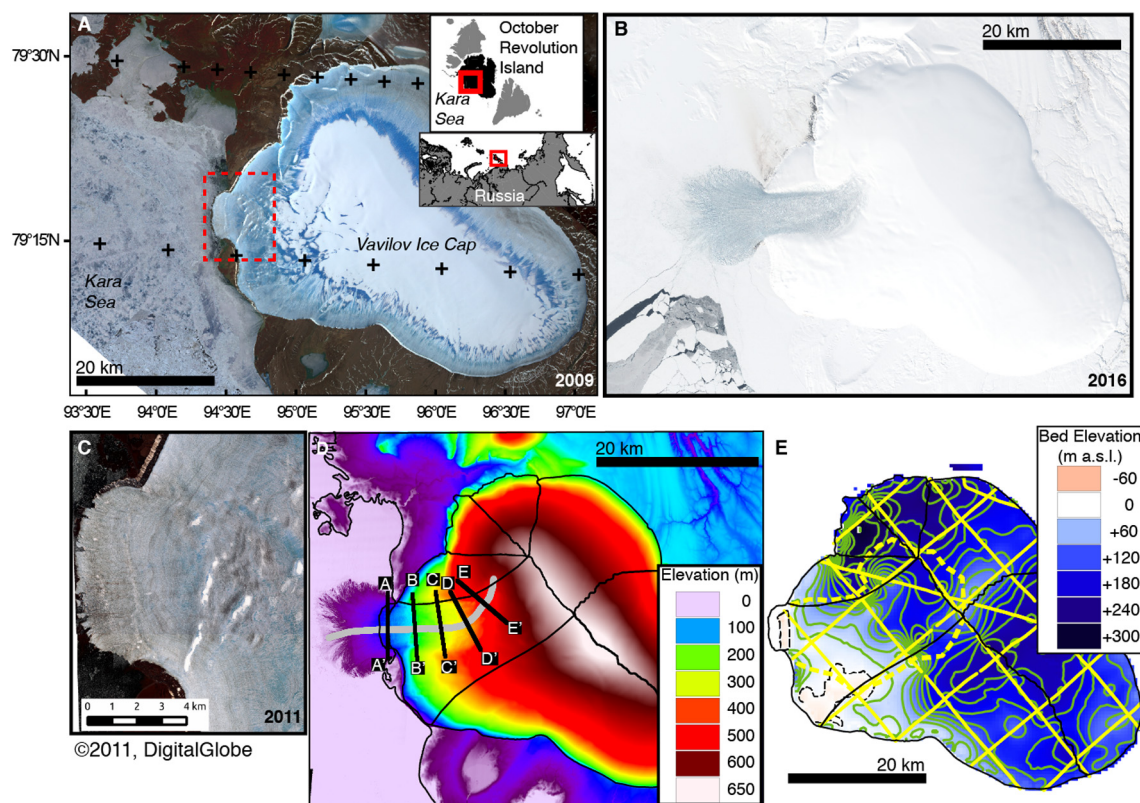
Fig. 1. Vavilov Ice Cap, Severnaya Zemlya Archipelago, Russian High Arctic. **A)** True color ASTER image from late summer, 2009: note front position and extent of summer melt. Red dotted box details region shown in C. Insets show location of Severnaya Zemlya and October Revolution Island (black). **B)** Landsat-8 true color image on May 8th 2016, note front position and crevasse field extending into the interior of the ice cap. **C)** Worldview-02 true color image showing front moraine, terminus position and continuous sediment bands in 2011. Image © 2011, DigitalGlobe, Inc. **D)** Elevation of Vavilov Ice Cap from spring 2016. Thin black lines – drainage basins from Randolf Glacier Inventory version-5 (Pfeffer et al., 2014). Thick grey line – centerline profile in Figs. 2, 3 and 4. Thick black lines – transverse profiles in Fig. 4. DEM created from DigitalGlobe Inc. stereo imagery. **E)** Bed elevation derived from airborne radio echo sounding. Green contours are 25 m intervals; dotted black contours are sea level, solid black basins outlines are from Randolf Glacier Inventory version-5. Yellow lines are flight lines used to collect radar echo sounding data; yellow dotted line is extent of crevassing in 2011 sub-meter optical imagery. Note scales in panels **A**, **B**, **D** and **E** are identical. (For interpretation of the colors in the figure(s), the reader is referred to the web version of this article.)

celeration and thinning but displays no previous surface evidence of surging (Dowdeswell and Williams, 1997), confirmed with high resolution imagery in Fig. 1c).

The ∼300 to 600 m thick, 1,820 km^2 Vavilov Ice Cap [Fig. 1] is frozen to its bed over the majority of its area, apart from a region along its western margin where basal sliding is potentially important for faster flow (Bassford et al., 2006a). Similar polythermal conditions are seen elsewhere in the Arctic (Gilbert et al., 2016). Ice-core drilling near the summit suggests the oldest ice at the base of the ice cap is Pleistocene age and shows the ice cap sits on top of frozen clay and sandstone deposits (Stiévenard et al., 1996). Palynological study of the ice core suggests precipitation at the ice cap became increasingly focused on the southwest side of the ice cap about 500 yrs ago (Andreev et al., 1997; Bassford et al., 2006b). Bassford et al. (2006b) suggest this change in precipitation pattern caused the western margin to advance slowly through time. During periods of intense melt the ice cap is stripped almost entirely of its snow cover and narrow supraglacial streams flow to the ice cap periphery. When intense melt occurs, continuous sediment bands in the ice can be traced in high resolution imagery at low elevation around the full periphery of the ice cap. At the western margin, these sediment bands are disturbed compared to elsewhere on the ice cap [Fig. 1C]. The disturbed but continuous bands coincide with the region of slightly faster ice flow and slow terminus advance.

Satellite radar interferometry from 1996 observed this western region of the ice cap moving at a peak rate of around 20 m/yr (∼5.4 cm/day), a rate at which modeling required some of the mo-

tion to be accommodated by basal sliding. The rest of the ice cap moved at speeds of less than 5 m/yr, consistent with internal deformation (Bassford et al., 2006b).

2. Results

In 2010, the ice in the western region started to accelerate. The front of this "fast" flow region was vertical and had a sediment apron, a configuration that is indicative of cold-based ice at the glacier front (Chin, 1991). In 2011 crevasses were observed from the western margin inland to within 5 km of the ∼700 m a.s.l. summit plateau of the ice cap using sub-meter resolution satellite imagery [Fig. 1]. The extent of the crevasses matches that of the inland extent of the ongoing ice acceleration and roughly coincides with an inherited, shallow sub-glacial valley [Fig. 1]. The increasingly rapid motion observed since 2010 requires a component of basal sliding. This motion may be accommodated by the plastic deformation of subglacial sediments or at the glacier-bed interface (Bassford et al., 2006b) or possibly due to enhanced deformation in Pleistocene ice (Gilbert et al., 2016) at the bottom of the ice cap, or at the boundary between Pleistocene and Holocene ice (Stiévenard et al., 1996).

From 1952 to 1985 the western part of the ice cap advanced around 400 m (∼12 m/yr) (Bassford et al., 2006b). The rate of advance accelerated significantly to ∼75 m/yr between 1998 and 2011. By 2000, the grounded ice front had moved offshore into the shallow Kara Sea pushing sediment before it. Rates of advance were steady between 2000 and 2009. By the spring of 2013 the
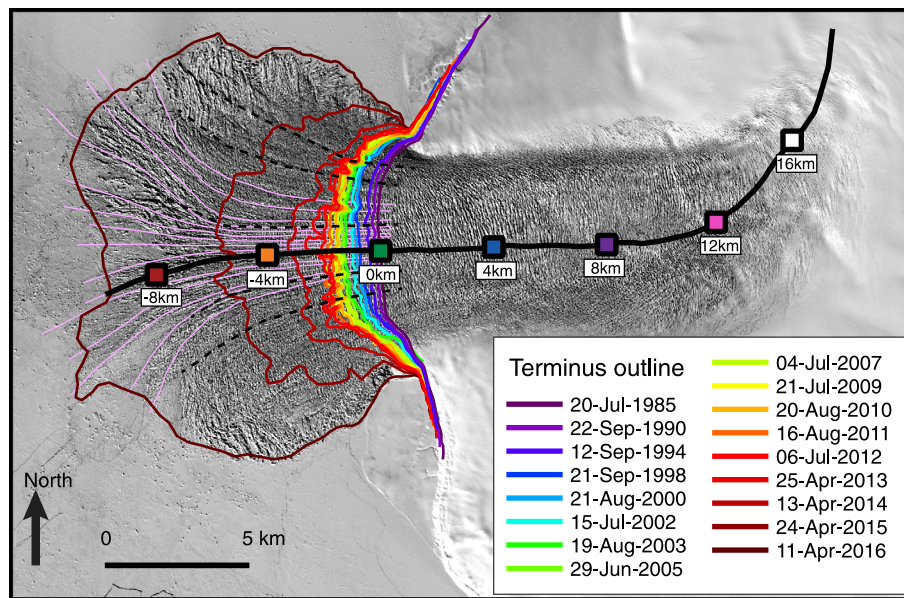
Fig. 2. Evolution of front position with time superimposed over Landsat-8 Panchromatic image from spring 2016. Black line is centerline flow-profile. Pink lines were used to calculate variability of advance in Fig. 3. Extents traced by hand. Black dotted lines show rough boundaries of flow units behaving like ice tongues. Noted numerical positions correspond to speed measurement locations along the centerline in Fig. 3, transverse thinning profiles in Fig. 4 and ASCAT sites in Extended data Fig. 2. Zero km is the position of the coastline before the glacier advanced, pre-1985.
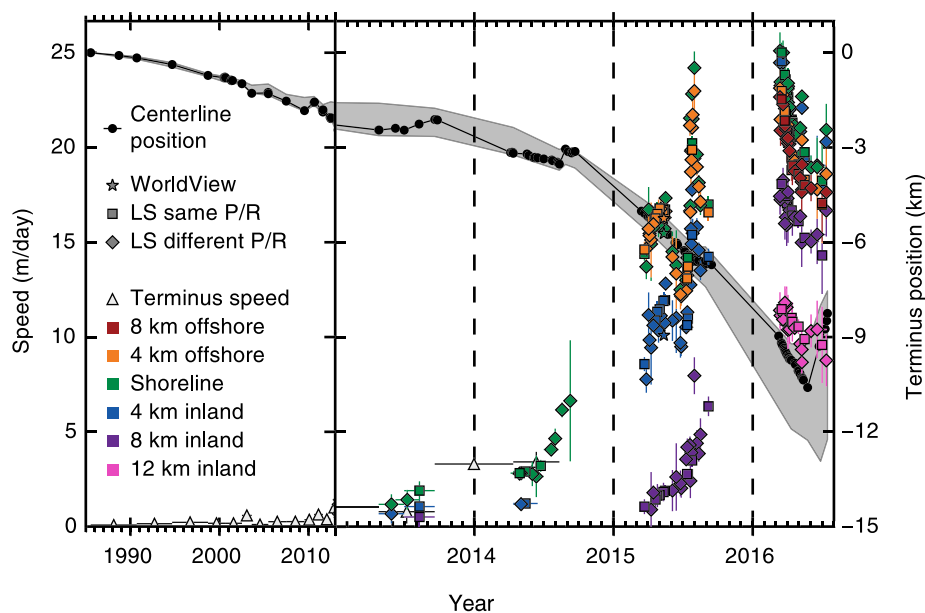

Fig. 3. Terminus position and ice speeds between 1985 and late 2016. Terminus position (black circles, right hand axis) show advance from the shoreline (0 km) until late 2016, when the front section of the glacier broke off. Ice advanced about 2 km between 1985 and late 2013. Rapid advance occurs between late 2014 and 2016. Grey envelope shows minimum and maximum ice advance based on the pink flowlines in Fig. 2. Terminus speeds between 1988 and 2013 are less than 50 m/yr. Very rapid speeds start in mid-2014 at the shoreline, with speeds reaching ∼25 m/day in late 2015, early 2016 at the same location. Inland speeds reach 10 m/day in 2016. Colored symbols are speeds through time at positions along the glacier centerline calculated using pixel-tracking on optical imagery. Stars indicate imagery source is WorldView, boxes are Landsat images from the same path and row, diamonds are Landsat images from different paths and rows. Uncertainties in speed are two sigma. Horizontal lines on speed points indicate interval between images which are often 8–24 days and too short to be seen on figure. Note change in X-axis scale.

terminal moraine at the front was absent. At this time the ice accelerated rapidly and started to form an unconfined marine-terminating piedmont glacier [Figs. 2, 3; Movie S1]. The bed beneath the offshore portion of the glacier is likely low-friction, saturated marine sediments similar to those commonly found offshore around other Arctic ice caps, such as those in Svalbard (Solheim, 1991). The front subsequently split and produced several grounded or partially grounded ice tongues that began to advance even more rapidly, at rates of more than 1000 m/yr between 2014 and 2015 [Figs. 2, 3]. The ice front may have achieved partial flotation (as revealed by a flattening of the profile of surface elevation, Fig. 4C)

when it advanced into the Kara Sea more than 5,000 m in the one-year period between April 2015 and April 2016 [Figs. 2, 3 and 4; Movie S1]. The reduction of resistive basal stresses and the rapid divergence of flow at the ice front led to a simultaneous speed up [Fig. 3] and steepening [Fig. 4] of the inland ice, where rates of motion accelerated to 9125 ± 354 m/yr (25.10 ± 0.97 m/day – uncertainties are 2 standard deviations) [Fig. 3].

We investigate the possibility that surface meltwater is able to penetrate to the glacier bed during summer melt periods, as seen at a cold-based ice cap in northern Greenland (Willis et al., 2015a) and as has been suggested to contribute to a surge event at the
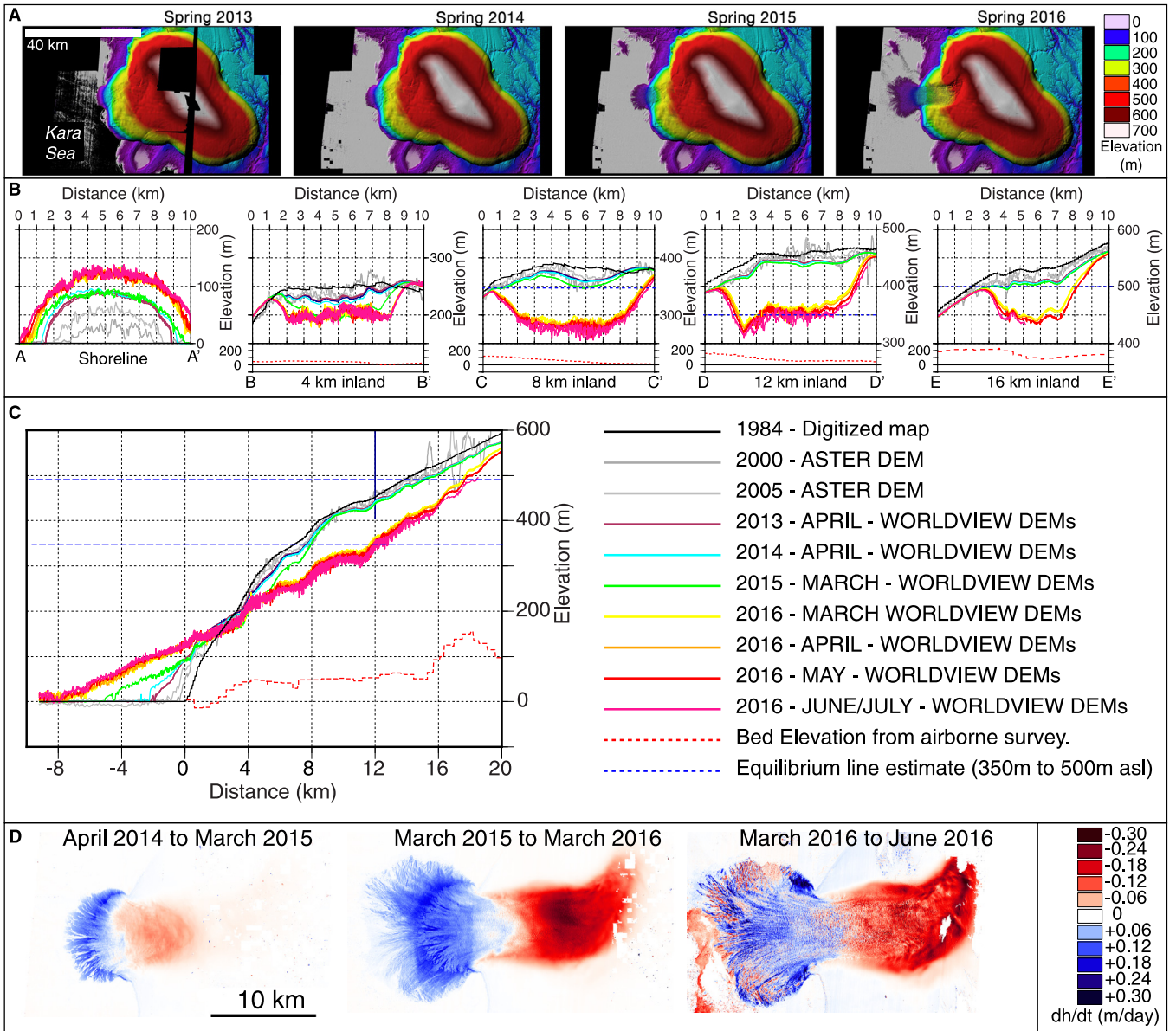
Fig. 4. Elevation changes at Vavilov Ice Cap, Russian High Arctic. **A)** Shaded Digital Surface Models from WorldView stereo imagery for Spring 2013 through 2016. The westward advance of the outlet glacier and propagation of thinning inland can be seen through time. DEMs created from DigitalGlobe Inc. stereo imagery; **B)** Profiles of elevation change perpendicular to the central flowline. The former shoreline at 0 km is on the left, then profiles every four kilometers inland extend to the right. Profile locations shown in Fig. 1D. Thickening occurs at the former shoreline, while large amounts of thinning occur inland between March 2015 and March 2016; **C)** Elevation profiles along centerline of glacier. 0 km is former shoreline. Bed elevation is red dotted line. Recent Worldview profiles are "noisier" due to observation of crevasse depths. The front advance offshore is clearly seen, as is the increased steepening of the ice surface at around 5 km inland, between 2014 and 2015. Large amounts of thinning are occurring far inland. Color key is the same as 4B. Blue dotted lines are estimated equilibrium line altitudes (Bassford et al., 2006c), below these heights the glacier is unlikely to regain mass in the future; **D)** Detailed plan views of rates of change of elevation through time from WorldView DEM differencing. The glacier is getting wider though time and is thinning inland at extraordinary rates of ~0.30 m/day. White gaps are areas of no data caused by blowing snow. DEMs created from DigitalGlobe Inc. stereo imagery.

more temperate Austfonna in Svalbard (Dunse et al., 2015). There are conflicting accounts of changes in surface meltwater at Vavilov Ice Cap. There are no exceptional air temperature anomalies that would drive the glacier dynamic changes [Dataset S1] from 2005 to mid-2016 at the Golomyanny weather station, near sea level approximately 80 km to the west, but climate data are not available on the ice cap, where conditions may be different. The yearly average temperature at Golomyanny is about $-12\,°C$ with peak summer temperatures of $+10\,°C$ and minimum winter temperatures of about $-40\,°C$. We note that the average amount of rainfall in 2011 and 2012 was larger than in the preceding 5 years [Dataset S1, Fig. S1].

Passive microwave observations of ice-surface wetness show 2011 and 2012 had extended melt seasons compared to previous years (Zhao et al., 2014). Sub-meter resolution optical satellite images from the melt seasons of 2009, 2011 and 2012 show bare ice over almost the entire ice cap, but that supraglacial runoff streams are narrow and supraglacial lakes are small, only a few square meters in area, and rare. Supraglacial meltwater might have been able to penetrate into the ice through existing crevasses and moulins and, if the water supply were constant, it may have reached the bed and helped precondition this region of the ice cap for rapid flow.

Fluctuations in ice motion [Fig. 3] in 2015 and 2016 are likely tied to an actively evolving drainage system at the ice bed, as observed in Greenland (Bartholomew et al., 2010; Moon et al., 2015, 2014; Stearns and van der Veen, 2018). Ice across the region accelerated by about 25% between late March of 2015 and late May

2015, before any melting had occurred at low elevation coastal portions of the ice cap. By mid June 2015 glacier speeds slowed as ice surface melting became more pervasive as temperatures at the Golomyanny station fluctuated around 0 °C [Fig. S1]. We assume this is because subglacial drainage became more efficient and organized. Ice velocity accelerated massively from late June through mid-July 2015 before slowing to springtime-like speeds again in August 2015 [Fig. S2]. We cannot observe winter ice velocity with optical sensors as the region is dark. A timeseries of SAR observations indicate a speed up occurred after late August 2015 (Strozzi et al., 2017). Our optically derived speeds [Fig. 3] match closely with the SAR observations. Our early springtime speeds in March of 2016 are between 50% and 100% faster than those we observe in late August of 2015 confirming the acceleration over winter, as previously observed by Strozzi et al. (2017). A winter speed up indicates that the supply of supraglacial meltwater to the base of the glacier system may be of secondary importance to the ice speeds in 2016 [Fig. 3], though it is possible that the cumulative effect of increased meltwater over multiple years had an effect.

Digital Elevation Models (DEMs) derived from sub-meter resolution satellite imagery are co-registered to ICESat returns over bedrock for the region and detail the remarkable evolution in ice-surface elevations between 2013 and 2016 [Fig. 4]. Ice height differences between a DEM produced by digitizing Russian military maps, sourced from aerial photos in 1984, and ICESat controlled DEMs produced in April 2013 show 10–30 m of thinning at altitudes of between 200 m and 600 m and an ice front advance of about 2.5 km over the 29-year interval. They show no evidence of excess mass or thickening in the accumulation area that would drive a kinematic wave downstream, a commonly observed surge mechanism at other glaciers (e.g. Sund et al., 2009). April 2013 to April 2014 shows a thickening of 30–50 m at the ice front, a slight advance and the formation of a prominent ice cliff. Inland there is virtually no difference in elevation profiles between 2013 and 2014. From April 2014 to April 2015 thinning of up to 50 m propagates about 8 km inland from the former coastline. The offshore ice front thickens considerably and the ice advances rapidly. Changes between April 2015 to April 2016 indicate full activation of the outlet glacier with thinning propagating to within 5 km of the summit region of the ice cap. The most pervasive thinning of more than 100 m/yr (∼0.30 m/day) occurs along the center flowline ∼11 km inland from the former coastline [Fig. 4D]. The surface-topographic expression of a small sub-glacial overdeepening near the former shoreline is apparent in the elevation profiles with the ice surface dropping upon entering the basin and then turning upwards at the downstream lip [Fig. 4C]. Transverse profiles [Fig. 4B] show a similar rapid acceleration in thinning between 2015 and 2016.

We investigate thinning rates and ice surface motions using knowledge of the bed geometry in an effort to gain insight into the broad-scale mechanisms controlling glacier motion. We calculate the stresses that drive and resist ice flow using the force budget method (Van Der Veen and Whillans, 1989). The force balance is calculated by rotating every pixel based on its velocity vector, with forces then determined in the along-flow direction. Resistance to flow can come from friction at the bed, from the sides, or from along-flow obstacles. Changes over time in the velocity field of a glacier should be explained by a subsequent change in the balance of forces controlling the flow.

Vavilov Ice Cap underwent a dramatic shift in its force balance between 2013 and 2016. In 2013, the driving stress was almost entirely balanced by basal drag, both of which show fairly uniform values of ∼100 kPa, except for in a small region just upstream from the former shoreline where lower stresses and some longitudinal stretching is seen (Fig. 5A). Contributions from lateral drag and longitudinal stress gradients are small during this time (Fig. 5A).

By 2015, basal drag along the trunk of the glacier drops to nearly zero, suggesting that the bed is well lubricated or highly mobile. The driving stresses along the trunk are almost entirely resisted by a combination of lateral drag and longitudinal stress gradients. The small area of low basal drag in 2013 expands to the north and south suggesting the addition of water from shear heating at the edges of the ice stream. The reduction of stress in this region cannot be attributed to infiltration of sea water as the bed is above sea level, and it is unlikely to be attributed to water from supraglacial sources as 2015 was a relatively normal year with very few supraglacial streams and ponds in the imagery. Fingers of high lateral drag values near the terminus of the glacier in 2015 indicate that the glacier remains grounded at the front. High values of driving stress and basal drag are propagating inland as the drawdown of interior ice causes steeper surface slopes (Fig. 5B).

By 2016, high values of driving stress and basal drag have propagated further inland and to the lateral margins where surface slopes are now high. Similar to an ice stream, the trunk of the glacier has low driving stresses, negligible basal drag values and attains very rapid speeds. Lateral drag and longitudinal stress gradients resist most of the driving stress along the trunk (Fig. 5C). These results show that up until 2013 the glacier was strongly supported by the bed. By 2015, the bed can no longer support the driving stresses, which are predominantly supported by longitudinal stress gradients and lateral drag. An extraordinary transition from a high friction bed to a near frictionless bed has taken place over just two years.

The geodetic mass balance of the grounded portion of the ice cap between 1984 and April 2013 is slightly negative at -0.04 ± 0.02 km^3/yr w.e. and is in agreement with modeled rates (Bassford et al., 2006c). Between April 2014 and April 2015 the mass balance is 21 times more negative, at -0.84 ± 0.004 km^3/yr w.e. Between 2015 and 2016 the mass loss is 5 times greater still at -4.48 ± 0.004 km^3/yr w.e. (∼100 fold increase on long-term rates). This is the single largest mass imbalance occurring in the Russian High Arctic; for comparison, the mass budget for the entire of the Russian Arctic region was -9.1 ± 2.0 km^3/yr w.e. between 2004 and 2009 (Moholdt et al., 2012). The 2015–2016 Vavilov rate equates to a loss of about 0.9% of the total volume of the 570 km^3 ice cap per year.

3. Discussion

Pan-Arctic radar observations of ice speeds indicate that glacier acceleration is becoming more common (Strozzi et al., 2017). Even within this context, the rate of ice loss at Vavilov is extreme. The area that is thinning (∼175 km^2) is relatively small but the total mass losses are more than half of those observed at the much larger 1,160 km^2 Basin-3 catchment at the Austfonna Ice Cap on Svalbard (McMillan et al., 2014). It is startling that the Vavilov Ice Cap, until recently an apparently stable ice cap with an almost entirely frozen bed that is almost entirely above sea level, is able to rapidly discharge such a large proportion of its ice in to the ocean in such a short period. The reduction in elevation and the ongoing widening of the inland portion of the outlet glacier [Fig. 4D] increases the area of the ice cap susceptible to melting below the equilibrium-line altitude. It is unlikely that the ice cap will recover mass in the warming climate, even with concomitant increases in precipitation, but this inference must be confirmed by future mass balance calculations.

The most rapid collapse of the Vavilov Ice Cap initiated as the ice front advanced over marine sediments into an unconfined bay that allowed spreading and stretching. The initial slow glacier advance was suggested by Bassford et al. (2006b) to be a legacy
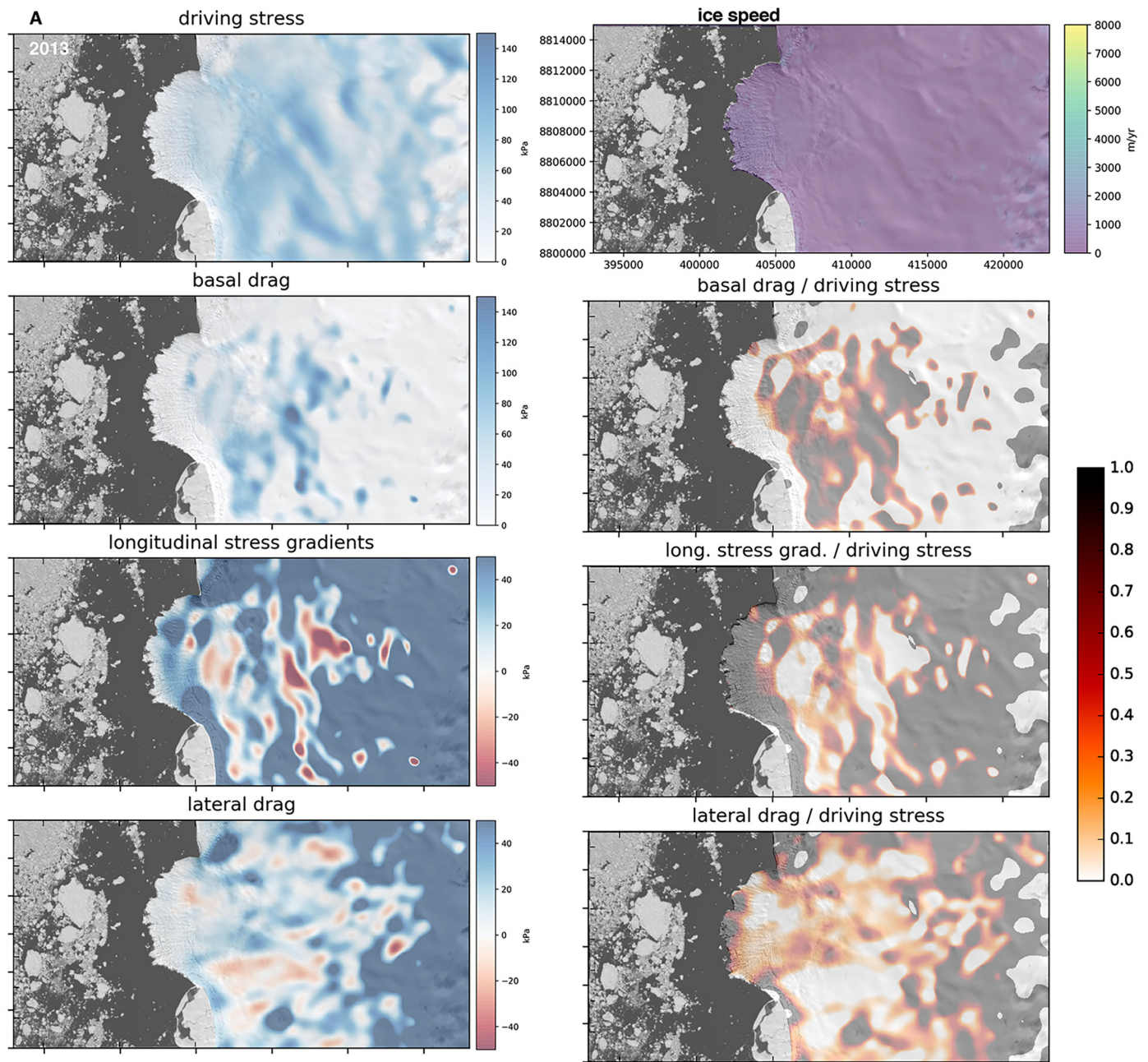
Fig. 5. Components of the force balance calculated using ice velocity and surface elevation data for **A)** 2013; **B)** 2015; and **C)** 2016. The left column shows the driving stress, and the three resistive stresses: basal drag, longitudinal stress gradients and lateral drag (positive values are resisting flow). The right column shows ice velocity (upper right), and the ratio of each resistive stress divided by the driving stress. Comparing the right-hand column in A, B and C highlights how the spatial patterns of resistive forces vary through time. Axes are in meters.

of the reorganization of the pattern of precipitation affecting the ice cap – a phenomenon of climate change that is often over-looked compared to changes in temperature in the polar regions. The slow advance could also be associated with small, unobserved changes in basal drag that would suggest the destabilization process at Vavilov is part of a very long duration process. The glacier advance was associated with long-term thinning at higher elevations [Figs. 3B, 4C] as expected, but the extraordinary acceleration after 2013 was not (Bassford et al., 2006b). During the subsequent rapid ice advance, continuity forced the inland ice to thin rapidly, accelerate and the areas at the margins to steepen dramatically.

We contend that the collapse of the ice cap has been driven by changing resistive stresses at the bed, and the effective de-buttressing, or removal of resistive stresses at the ice front. Precon-ditioning of the ice for rapid flow by internal warming caused by the percolation and refreezing of surface water (Dunse et al., 2015; Willis et al., 2015a) in 2009, 2011 and 2012 is plausible, but the massive acceleration of the inland ice over the 2015–2016 win-ter suggests that an active supply of supraglacial meltwater to the bed of the glacier is not a controlling factor. The thermal regime and bed interface properties most likely control this rapid ice mo-tion, with high speeds promoting strain softening (Schoof, 2004; Schoof and Hewitt, 2013; Suckale et al., 2014) at the shearing boundary between stationary and fast moving ice, and friction at the bed and shear margins promoting water production. This basal water, at lithostatic pressure, may have infiltrated and mobilized the clays and till beneath the ice cap, contributing further to the extraordinary sliding speeds (Iverson et al., 1998).
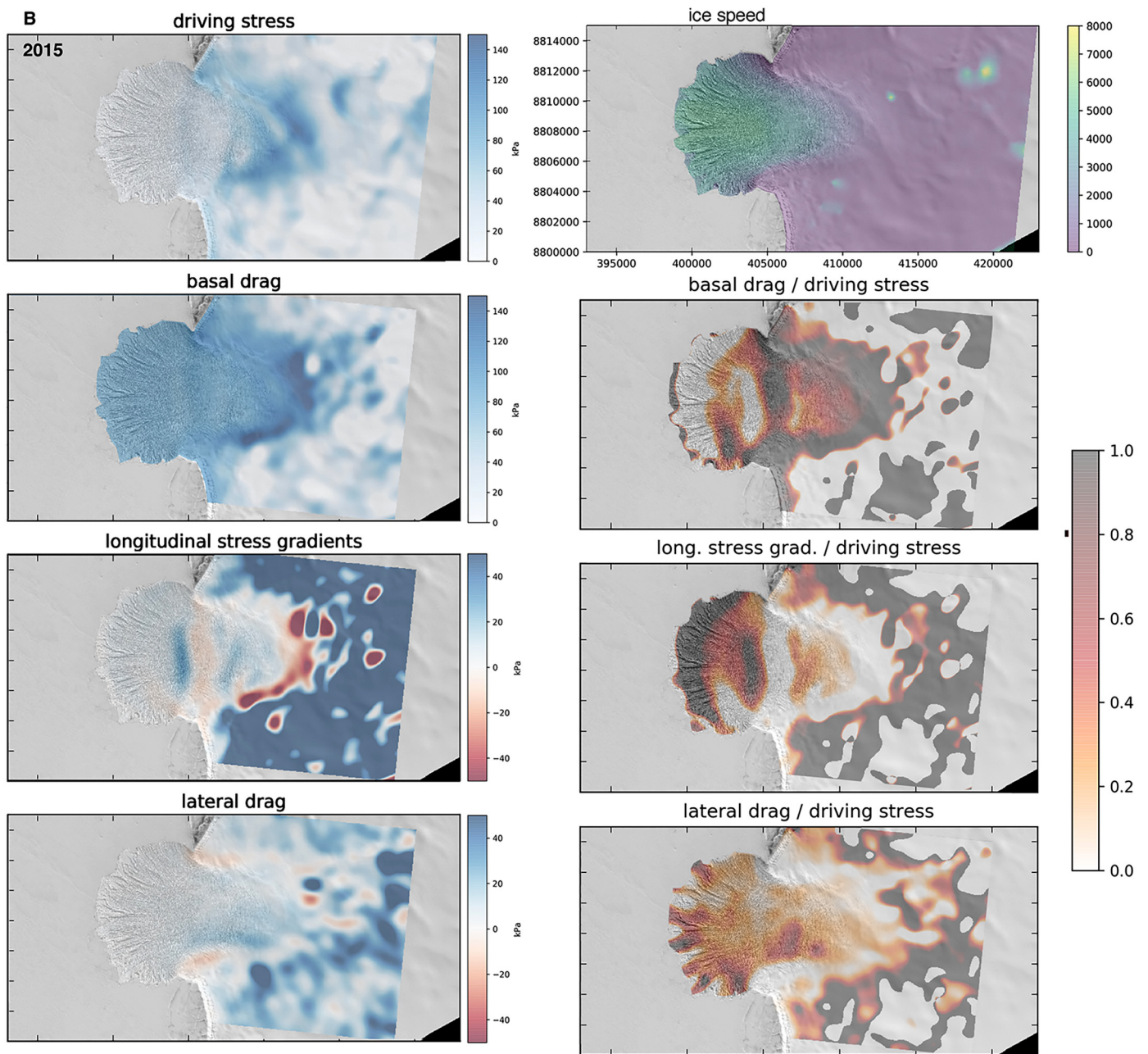
Fig. 5. (*continued*)

4. Material and methods

It is surprising that a previously stable ice cap like Vavilov can lose mass in such a dramatic manner, as marine terminating cold- and polythermal based ice caps and ice sheets with sub-glacial bed elevations that are above sea level are often thought to be insulated from rapid accelerations and dynamic changes. It has long been recognized that marine-terminating glaciers with reverse-bed slopes and bed elevations well below sea level can experience instabilities that propagate inland, triggering collapse (DeConto and Pollard, 2016). There is, however, a general acceptance that ice caps in the polar regions will only respond slowly to a warming climate and changes in boundary conditions. Our observations indicate this assumption should be questioned, especially when glaciers can advance over low friction sediments. We show polar glaciers that have bed elevations above sea level can rapidly collapse. This has ramifications for glaciers elsewhere in the polar regions and especially for those fringing Antarctica and Greenland, many of which are above sea level and are therefore assumed to be stable.

Ice depths were measured using helicopter-borne radar echo sounding. Full details of the method can be found in (Dowdeswell et al., 2002). Surface Elevations from WorldView DEMs were derived using the Ames Stereo Pipeline applied to half-meter resolution imagery (Shean et al., 2016). We independently co-register DEMs using filtered and cleaned NASA ICESat lidar returns (Moholdt et al., 2010) over nearby bedrock. The robust mean of the smallest 75% percentile fit between WorldView derived DEMs and the ICESat over bedrock are typically better than 0.35 m, ASTER results are 20 times noisier (Table S1). When performing volume calculations, we add the ICESat uncertainty to the DEM uncertainties in quadrature and assume an ice density of 900 kg/m^3. All ICESat-corrected DEMs are available as 32-bit geotiff files at the Polar Geospatial Center of the University of Minnesota. Elevations from 1984 are taken from a 90 m posting
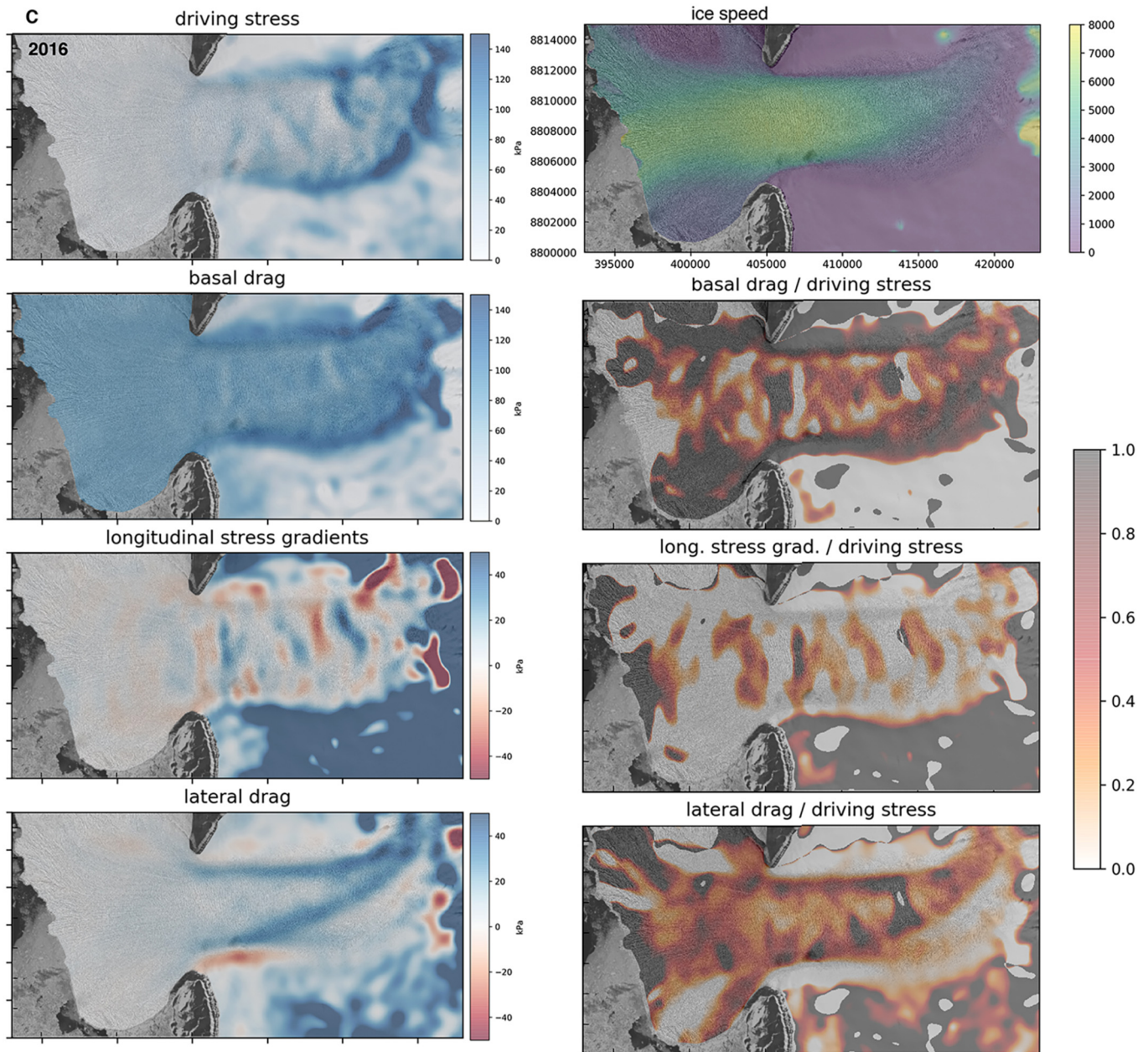
Fig. 5. (*continued*)

DEM compiled from Russian military maps and available at the www.viewfinderpanorama.org website. Uncertainties on this product when compared to ICESat in the Vavilov region are ± 10.0 m, see (Willis et al., 2015b). Ice motions are derived using the ampcor pixel-tracking module from ROI_PAC (Rosen et al., 2004). This normalized cross-correlation routine determines the peak on a correlation surface generated from a co-registered satellite image pair (Willis et al., 2012). Seventy-nine pairs of Landsat 8 Operational Land Imager (OLI) panchromatic (band 8, 15 m pixel size) images and 1 pair of WorldView-01 panchromatic (0.5 m pixel size) are processed. To improve the quality of the correlation surface, we apply a gaussian high-pass filter and a square-root stretch function to each raw image. We correct for mis-registration by calculating the median offset over exposed bedrock regions, which should be zero, and subtract this from pixel-tracking results. The corrected results are smoothed, masking local outliers. Uncertainties are calculated as the standard deviation of bedrock offset. We used ESA Advanced Scatterometer (ASCAT) vertically polarized all-pass (msfa) microwave data with a local effective time of day generated from multiple overpasses of the Arctic region. Data were processed using the scatterometer image reconstruction (SIR) algorithm with filtering (Drinkwater et al., 1994; Early and Long, 2001). Data used were in sigma naught at 40 degree incidence. Data are at 4.45 km resolution due the multiple overpasses, yielding higher spatial resolution but compromising on temporal frequency. Enhanced resolution SIR data were provided by the Brigham Young University MERS Laboratory [http://www.scp.byu.edu/data/Ascat/SIR/msfa/Arc.html]. Daily data were concatenated into a time series shown for select pixels on the Vavilov Ice Cap (Fig S2). The dramatic drop in sigma naught indicates high probability of surface snow melt.

Appendix A. Supplementary material

Supplementary material related to this article (Dataset S1, Table S1, Figs. S1 and S2, Movie S1) can be found online at https://doi.org/10.1016/j.epsl.2018.08.049.

References

Andreev, A., Nikolaev, V., Boi'sheiyanov, D., Vladimir, P., 1997. Pollen and isotope investigations of an ice core from Vavilov Ice Cap, October Revolution Island, Severnaya Zemlya Archipelago, Russia. Géogr. Phys. Quat. 51, 379–389.

Bartholomew, I., Nienow, P., Mair, D., Hubbard, A., King, M.A., Sole, A., 2010. Seasonal evolution of subglacial drainage and acceleration in a Greenland outlet glacier. Nat. Geosci. 3, 408–411. https://doi.org/10.1038/ngeo863.

Bassford, R.P., Siegert, M.J., Dowdeswell, J.A., 2006a. Quantifying the mass balance of ice caps on Severnaya Zemlya, Russian High Arctic. III: Sensitivity of ice caps in Severnaya Zemlya to future climate change. Arct. Antarct. Alp. Res. 38, 21–33. https://doi.org/10.1657/1523-0430(2006)038[0021:QTMBOI]2.0.CO;2.

Bassford, R.P., Siegert, M.J., Dowdeswell, J.A., 2006b. Quantifying the mass balance of ice caps on Severnaya Zemlya, Russian High Arctic. II: Modeling the flow of the Vavilov Ice Cap under the present climate. Arct. Antarct. Alp. Res. 38, 13–20. https://doi.org/10.1657/1523-0430(2006)038[0013:QTMBOI]2.0.CO;2.

Bassford, R.P., Siegert, M.J., Dowdeswell, J.A., Oerlemans, J., Glazovsky, A.F., Macheret, Y.Y., 2006c. Quantifying the mass balance of ice caps on Severnaya Zemlya, Russian High Arctic. I: Climate and mass balance of the Vavilov Ice Cap. Arct. Antarct. Alp. Res. 38, 1–12. https://doi.org/10.1657/1523-0430(2006)038[0021:QTMBOI]2.0.CO;2.

Bindschadler, R., Harrison, W.D., Raymond, C.F., Gantet, C., 1976. Thermal regime of a surge-type glacier. J. Glaciol. 16, 251–259. https://doi.org/10.3189/S0022143000031579.

Chin, T.J.H., 1991. Polar glacier margin and debris features. In: Memorie della Societa Geologica Italiana – Proceedings of the Meeting on Earth Sciences in Antarctica. Siena, Italy, pp. 25–44.

Clarke, G.K.C., 1991. Length, width and slope influences on glacier surging. J. Glaciol. 37, 236–246. https://doi.org/10.1017/S0022143000007255.

Copland, L., Sharp, M.J., Dowdeswell, J.A., 2003. The distribution and flow characteristics of surge-type glaciers in the Canadian High Arctic. Ann. Glaciol.. https://doi.org/10.3189/172756403781816301.

DeConto, R.M., Pollard, D., 2016. Contribution of Antarctica to past and future sea-level rise. Nature 531, 591–597. https://doi.org/10.1038/nature17145.

Dowdeswell, J.A., Bassford, R.P., Gorman, M.R., Williams, M., Glazovsky, A.F., Macheret, Y.Y., Shepherd, A.P., Vasilenko, Y.V., Savatyuguin, L.M., Hubberten, H.W., Miller, H., 2002. Form and flow of the Academy of Sciences Ice Cap, Severnaya Zemlya, Russian High Arctic. J. Geophys. Res., Solid Earth 107. https://doi.org/10.1029/2000JB000129.

Dowdeswell, J.A., Williams, M., 1997. Surge-type glaciers in the Russian High Arctic identified from digital satellite imagery. J. Glaciol. 43, 489–494. https://doi.org/10.1017/S0022143000035097.

Drinkwater, M.R., Long, D.G., Early, D.S., 1994. Enhanced-resolution ERS-1 scatterometer imaging of Antarctic ice. Earth Obs. Q. 43, 4–6.

Dunse, T., Schellenberger, T., Hagen, J.O., Kääb, A., Schuler, T.V., Reijmer, C.H., 2015. Glacier-surge mechanisms promoted by a hydro-thermodynamic feedback to summer melt. Cryosphere. https://doi.org/10.5194/tc-9-197-2015.

Early, D.S., Long, D.G., 2001. Image reconstruction and enhanced resolution imaging from irregular samples. IEEE Trans. Geosci. Remote Sens. 39, 291–302. https://doi.org/10.1109/36.905237.

Gardner, A.S., Moholdt, G., Cogley, J.G., Wouters, B., Arendt, A.A., Wahr, J., Berthier, E., Hock, R., Pfeffer, W.T., Kaser, G., Ligtenberg, S.R.M., Bolch, T., Sharp, M.J., Hagen, J.O., van den Broeke, M.R., Paul, F., 2013. A reconciled estimate of glacier contributions to sea level rise: 2003 to 2009. Science 80 (340), 852–857. https://doi.org/10.1126/science.1234532.

Gilbert, A., Flowers, G.E., Miller, G.H., Rabus, B.T., Van Wychen, W., Gardner, A.S., Copland, L., 2016. Sensitivity of Barnes Ice Cap, Baffin Island, Canada, to climate state and internal dynamics. J. Geophys. Res., Earth Surf. https://doi.org/10.1002/2016JF003839.

Grant, K.L., Stokes, C.R., Evans, I.S., 2009a. Identification and characteristics of surge-type glaciers on Novaya Zemlya, Russian Arctic. J. Glaciol. 55, 960–972.

Grant, K.L., Stokes, C.R., Evans, I.S., 2009b. Identification and characteristics of surge-type glaciers on Novaya Zemlya, Russian Arctic. J. Glaciol. https://doi.org/10.3189/002214309790794940.

Harrison, W.D., Post, A.S., 2003. How much do we really know about glacier surging? Ann. Glaciol. 36, 1–6. https://doi.org/10.3189/172756403781816185.

Iverson, N.R., Hoover, T.S., Baker, R.W., 1998. Ring-shear studies of till deformation: Coulomb-plastic behavior and distributed strain in glacier beds. J. Glaciol. https://doi.org/10.1017/S0022143000002136.

Jiskoot, H., Murray, T., Boyle, P., 2000. Controls on the distribution of surge-type glaciers in Svalbard. J. Glaciol. 46, 412–422. https://doi.org/10.3189/172756500781833115.

Kamb, B., Raymond, C.F., Harrison, W.D., Engelhardt, H., Echelmeyer, K.A., Humphrey, N., Brugman, M.M., Pfeffer, T., 1985. Glacier surge mechanism: 1982–1983 surge of variegated glacier, Alaska. Science 80 (227), 469–479. https://doi.org/10.1126/science.227.4686.469.

McMillan, M., Shepherd, A., Gourmelen, N., Dehecq, A., Leeson, A., Ridout, A., Flament, T., Hogg, A., Gilbert, L., Benham, T., Van Den Broeke, M., Dowdeswell, J.A., Fettweis, X., Noël, B., Strozzi, T., 2014. Rapid dynamic activation of a marine-based Arctic ice cap. Geophys. Res. Lett. 41, 8902–8909. https://doi.org/10.1002/2014GL062255.

Moholdt, G., Nuth, C., Hagen, J.O., Kohler, J., 2010. Recent elevation changes of Svalbard glaciers derived from ICESat laser altimetry. Remote Sens. Environ. 114, 2756–2767. https://doi.org/10.1016/j.rse.2010.06.008.

Moholdt, G., Wouters, B., Gardner, A.S., 2012. Recent mass changes of glaciers in the Russian High Arctic. Geophys. Res. Lett. 39. https://doi.org/10.1029/2012GL051466.

Moon, T., Joughin, I., Smith, B., 2015. Seasonal to multiyear variability of glacier surface velocity, terminus position, and sea ice/ice mélange in northwest Greenland. J. Geophys. Res., Earth Surf. 120. https://doi.org/10.1002/2015JF003494.

Moon, T., Joughin, I., Smith, B., Van Den Broeke, M.R., Van De Berg, W.J., Noël, B., Usher, M., 2014. Distinct patterns of seasonal Greenland glacier velocity. Geophys. Res. Lett. 41, 7209–7216. https://doi.org/10.1002/2014GL061836.

Murray, T., Strozzi, T., Luckman, A., Jiskoot, H., Christakos, P., 2003. Is there a single surge mechanism? Contrasts in dynamics between glacier surges in Svalbard and other regions. J. Geophys. Res., Solid Earth 108. https://doi.org/10.1029/2002JB001906.

Ottesen, D., Dowdeswell, J.A., 2006. Assemblages of submarine landforms produced by tidewater glaciers in Svalbard. J. Geophys. Res., Earth Surf. https://doi.org/10.1029/2005JF000330.

Ottesen, D., Dowdeswell, J.A., Bellec, V.K., Bjarnadóttir, L.R., 2017. The geomorphic imprint of glacier surges into open-marine waters: examples from eastern Svalbard. Mar. Geol. https://doi.org/10.1016/j.margeo.2017.08.007.

Pfeffer, W.T., Arendt, A.A., Bliss, A., Bolch, T., Cogley, J.G., Gardner, A.S., Hagen, J.O., Hock, R., Kaser, G., Kienholz, C., Miles, E.S., Moholdt, G., Mölg, N., Paul, F., Radić, V., Rastner, P., Raup, B.H., Rich, J., Sharp, M.J., Andreassen, L.M., Bajracharya, S., Barrand, N.E., Beedle, M.J., Berthier, E., Bhambri, R., Brown, I., Burgess, D.O., Burgess, E.W., Cawkwell, F., Chinn, T., Copland, L., Cullen, N.J., Davies, B., De Angelis, H., Fountain, A.G., Frey, H., Giffen, B.A., Glasser, N.F., Gurney, S.D., Hagg, W., Hall, D.K., Haritashya, U.K., Hartmann, G., Herreid, S., Howat, I., Jiskoot, H., Khromova, T.E., Klein, A., Kohler, J., König, M., Kriegel, D., Kutuzov, S., Lavrentiev, I., Le Bris, R., Li, X., Manley, W.F., Mayer, C., Menounos, B., Mercer, A., Mool, P., Negrete, A., Nosenko, G., Nuth, C., Osmonov, A., Pettersson, R., Racoviteanu, A., Ranzi, R., Sarikaya, M.A., Schneider, C., Sigurdsson, O., Sirguey, P., Stokes, C.R., Wheate, R., Wolken, G.J., Wu, L.Z., Wyatt, F.R., 2014. The Randolph Glacier Inventory: a globally complete inventory of glaciers. J. Glaciol. 60. https://doi.org/10.3189/2014JoG13J176.

Radić, V., Bliss, A., Beedlow, A.C., Hock, R., Miles, E., Cogley, J.G., 2014. Regional and global projections of twenty-first century glacier mass changes in response to climate scenarios from global climate models. Clim. Dyn. 42, 37–58. https://doi.org/10.1007/s00382-013-1719-7.

Raymond, C.F., 1987. How do glaciers surge? A review. J. Geophys. Res. 92, 9121. https://doi.org/10.1029/JB092iB09p09121.

Rosen, P.A., Hensley, S., Peltzer, G., Simons, M., 2004. Updated repeat orbit interferometry package released. Eos 85, 47. https://doi.org/10.1029/2004EO050004.

Schoof, C., 2004. On the mechanics of ice-stream shear margins. J. Glaciol. 50. https://doi.org/10.3189/acprof:oso/9780199556861.003.0007.

Schoof, C., Hewitt, I., 2013. Ice-sheet dynamics. Annu. Rev. Fluid Mech. 45, 217–239. https://doi.org/10.1146/annurev-fluid-011212-140632.

Sevestre, H., Benn, D.I., 2015. Climatic and geometric controls on the global distribution of surge-type glaciers: implications for a unifying model of surging. J. Glaciol. 61, 646–662. https://doi.org/10.3189/2015JoG14J136.

Shean, D.E., Alexandrov, O., Moratto, Z.M., Smith, B.E., Joughin, I.R., Porter, C., Morin, P., 2016. An automated, open-source pipeline for mass production of digital elevation models (DEMs) from very-high-resolution commercial stereo

satellite imagery. ISPRS J. Photogramm. Remote Sens. 116, 101–117. https://doi.org/10.1016/j.isprsjprs.2016.03.012.

Solheim, A., 1991. The depositional environment of surging sub-polar tidewater glaciers: a case study of the morphology, sedimentation and sediment properties in a surge affected marine basin outside Nordaustlandet, the northern Barents Sea, 194.

Stearns, L.A., van der Veen, C.J., 2018. Friction at the bed does not control fast glacier flow. Science 80.

Stiévenard, M., Nikolaëv, V., Bol'shiyanov, D.Y., Fléhoc, C., Jouzel, J., Klementyev, O.L., Souchez, R., 1996. Pleistocene ice at the bottom of the Vavilov ice cap, Severnaya Zemlya, Russian Arctic. J. Glaciol. https://doi.org/10.1017/S0022143000003385.

Strozzi, T., Paul, F., Wiesmann, A., Schellenberger, T., Kääb, A., 2017. Circum-Arctic changes in the flow of glaciers and ice caps from satellite SAR data between the 1990s and 2017. Remote Sens. 9, 1004–1025. https://doi.org/10.3390/rs9090947.

Suckale, J., Platt, J.D., Perol, T., Rice, J.R., 2014. Deformation-induced melting in the margins of the West Antarctic ice streams. J. Geophys. Res., Earth Surf. 119, 1004–1025. https://doi.org/10.1002/2013JF003008.

Sund, M., Eiken, T., Hagen, J.O., Kääb, A., 2009. Svalbard surge dynamics derived from geometric changes. Ann. Glaciol. 50, 50–60. https://doi.org/10.3189/172756409789624265.

Van Der Veen, C.J., Whillans, I.M., 1989. Force budget: I. Theory and numerical methods. J. Glaciol. 35, 53–60. https://doi.org/10.3189/002214389793701581.

Willis, M.J., Herried, B.G., Bevis, M.G., Bell, R.E., 2015a. Recharge of a subglacial lake by surface meltwater in northeast Greenland. Nature 518, 223–227. https://doi.org/10.1038/nature14116.

Willis, M.J., Melkonian, A.K., Pritchard, M.E., 2015b. Outlet glacier response to the 2012 collapse of the Matusevich Ice Shelf, Severnaya Zemlya, Russian Arctic. J. Geophys. Res., Earth Surf. 120, 2040–2055. https://doi.org/10.1002/2015JF003544.

Willis, M.J., Melkonian, A.K., Pritchard, M.E., Ramage, J.M., 2012. Ice loss rates at the Northern Patagonian Icefield derived using a decade of satellite remote sensing. Remote Sens. Environ. 117, 184–198. https://doi.org/10.1016/j.rse.2011.09.017.

Zhao, M., Ramage, J., Semmens, K., Obleitner, F., 2014. Recent ice cap snowmelt in Russian High Arctic and anti-correlation with late summer sea ice extent. Environ. Res. Lett. 9. https://doi.org/10.1088/1748-9326/9/4/045009.